Pathan Amjadkhan Noorkhan, Sangshetty Kalayne / International Journal of Engineering Research and Applications (IJERA) ISSN: 2248-9622 www.ijera.com
Vol. 2, Issue 4, June-July 2012, pp.681-685

Synthesis, Characterization Ac Conductivity Of Nickel Ferrite

Pathan Amjadkhan Noorkhan[1] and Sangshetty Kalayne[2*]
[1]Department of Physics, Singhania University, Pacheri- Bari, JhunJunnu, Rajasthan
[2]Department of Physics, Bheemanna Khandre Institute of Technology (REC), Bhalki, Bidar, Karnataka, India.

Abstract

Nickel ferrites were synthesized by employing sol gel technique at 600^{0}C sintering temperature. The prepared samples were characterized by XRD for structural analysis indicates that the percentage of iron ions in B site increases, the intensity of the (222) peak increases. This indicates that the structural changes of the $NiFe_3O_4$, arise from the shifting of ions between A and B sites. The morphology was studies using SEM and found that morphology is more favorable for charge transportation in ferrites. The nickel ferrite ($NiFe_3O_4$) shows high σ_{ac} conductivity due to dipole polarization. The high value of dielectric constant of the sample $NiFe_3O_4$ is because of structural changes associated with the nickel ferrite when the grain size is reduced to nanometer order.

Key words: Nickel ferrite, X-ray diffraction, Ac conductivity, dielectric constant.

Introduction

Mixed nickel ferrites having high Curie temperature and different magnetization form an important class of magnetic materials used in many technological applications [1]. Those characteristics are in close connection with the magnetic structure, which is dependent on the magnetic cations, their distribution and concentration. Ni–Zn ferrites, which have a high resistivity and low eddy current loss, are used in high frequency and pulse field applications. This system has a cubic spinel crystal structure with the unit cell consisting of eight formula units of the form $Znx^{2+}Fe_{1-x}^{3+}[Ni_{1-x}^{2+}Fe_{1+x}^{3+}]O_4^{2-}$. The 32 oxygen anions per unit cell form a face centered cubic cage, while the metallic cations occupy interstices. The metallic cations outside the bracket occupy the tetrahedral sites (A-sites) comprising tetrahedral sublattice while those metallic cationsenclosed by the bracket occupy octahedral sites (B-sites) comprising the octahedral sublattice [2-3]. The properties of ferrites are very sensitive to the method of preparation and the amount and type of substitution. The addition of impurities induces changes in the defect structure and texture of the crystal. An understanding of the mechanisms involved in the changes caused by the addition of impurities provides information on which the reliable formulation of ferrites suitable for specific applications can be based.

Ceramic method [4, 5] for the preparation of ferrites places certain limitations such as, requirement of relatively high firing temperature and more time which may cause the evaporation of certain elements like Zn [6] leading to the formation of chemically inhomogeneous material [7]. In case of Ni Zn ferrites, zinc volatilization at high temperature increases the electron hopping and reduces resistivity [8, 9]. During milling and grinding, there may be a loss of some material, which leads to nonstoichiometry in the final product [10]. Also the ferrites prepared by ceramic method have the larger particle size and low density. Chemical method overcomes these limitations of ceramic method and makes it possible to prepare the homogeneous, dense and smaller particle size ferrite [11, 12].

Among the spinel type ferrites, nickel ferrite is a suitable material for microwave applications [13]. It is noted for its high Curie temperature and good temperature stability of saturation magnetization [14].

The properties of nanoparticles are interesting due to the presence of very large and highly disordered grain boundaries. Because of the peculiarities of the grain boundaries nanomaterials exhibit unusual and/or enhanced dielectric properties. In this present paper authors report the synthesis, characterization, ac conductivity and dielectric properties of nickel ferrite.

Experimental

All Chemicals used were analytical grade (AR). The nickel chloride (purity 99.99%) and dehydrated ferric chloride were procured and were used as received.

Nickel chloride and ferric chloride are mixed in calculated stoichiometric with oxalic acid in equimolar ratio so as to form nickel ferric oxalate precursor. The precursor is then filtered and dried at 50^{0}C to achieve constant weight. The precursor is mixed with polyethylene glycol (PEG) in the ratio 1:5 and is ignited. The combustion propagates throughout the precursor. After completion of combustion nickel

ferrite ($NiFe_3O_4$) is formed. The nickel ferrite is sonicated in acetone media for 20min and then calcinated at 600^0C to remove the impurities. Finally, fine graded nanosized nickel ferrite particles are formed.

The pellets of 10 mm diameter are prepared with thickness varying up to 2 mm by applying pressure of 10 Tons in a UTM – 40 (40 Ton Universal testing machine). For temperature dependent conductivity and sensor studies, the pellets are coated with silver paste on either side of the surfaces to obtain better contacts.

The X-ray diffraction (XRD) pattern of the $NiFe_3O_4$ was recorded at room temperature by employing an x-ray powder diffractometer (Rigaku Miniflex) with CuK_α radiation (α=1.5405A^0) in the 2θ (Bragg angles) range ($2^0 \leq 2\theta \leq 10^0$) at a scan speed of 0.5^0 minute^{-1}.

The percentage transmittances for the entire sample are measured from 300 to 4000 cm^{-1}. The SEM images of polyaniline cadmium oxide composites were recorded using Philips XL-30 (ESEM) scanning electron microscopy. The set up used for measuring ac conductivity is Hioki 3050 impedance analyzer, which is in turn interfaced to the computer.

Results and discussion

An analysis of the dielectric properties of the $NiFe_3O_4$ has been carried out using impedance spectroscopy on application of a small a. c. signal across the sample cell with blocking electrode (stainless steel). Complex impedance parameters (i.e., capacitance, dissipation factor, impedance, phase angles parameters) were measured with a computer-controlled impedance analyzer **(**HIOKI LCR Hi-Tester, Model: 3532, Japan). A. C. conductivity has been evaluated from dielectric data in accordance with the relation:

$$\sigma_{ac} = \omega\varepsilon_0\varepsilon r\tan\delta$$

where ε_r = C/C0 is the relative permittivity, tanδ = tangent loss factor, C_0 = vacuum capacitance of the cell. The real and imaginary part of permittivity and modulus was calculated from the relation

Figure 1 shows the XRD patterns of $NiFe_3O_4$ at600^{o}C sintering temperature. The peaks in the spectra agreed closely with the data in the ICDD file (card number 10-325) for $Ni_XFe_{X-1}O_4$ indicating that the samples synthesized were nickel ferrite. The diffraction pattern of the samples showed broad peaks when compared with the bulk nickel ferrite. The average grain sizes of the particles were calculated from the full width at half maximum (FWHM) values of (311) reflection of the X-ray diffraction using Scherrer's equation (Klug and Alexander 1954).

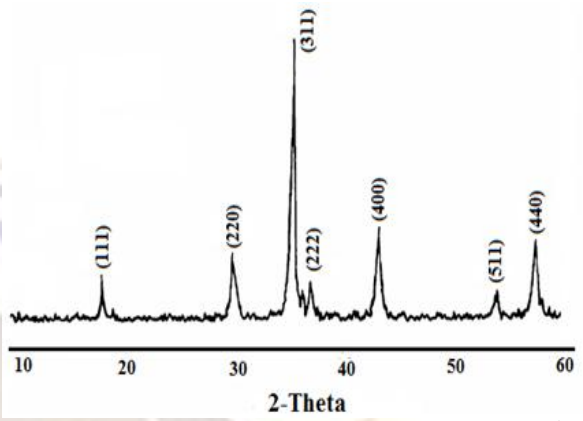

Figure 1. Shows the XRD pattern of $NiFe_3O_4$ at 600^{o}C sintering temperature

Figure 1show the XRD pattern of $NiFe_3O_4$ at 600^{o}C sintering temperature. It was reported that nickel ferrite deviates from its inverse spinel structure with the reduction in grain size by Ponpandian et al. When the grain size of nickel ferrite is reduced to nanometer order, some percentage of nickel ions get shifted from B site to A site at the same time shifting an equal number of iron ions from A to B site. The percentage of iron ions in B site increases with the reduction in grain size. This shifting of ions causes changes in XRD pattern also. As the percentage of iron ions in B site increases, the intensity of the (222) peak increases. This indicates that the structural changes of the $NiFe_3O_4$, arise from the shifting of ions between A and B sites. This shifting of ions is assumed to be prominent near the surface layers. Because the arrangement of ions in the core region of nanoparticles is identical with that in bulk crystals, while the altered structure due to the reduction in the size is confined to surface layers. As the size of a particle is reduced the surface to volume ratio increases and the number of iron ions in B sites increases.

Scanning Electron Microscope (SEM)

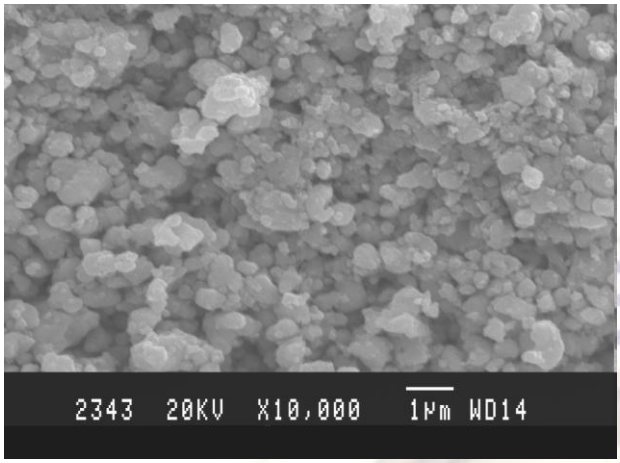

Figure 2. Shows that the SEM image of $Ni_XFe_{X-1}O_4$ at 600°C sintering temperature

Figure 2 (a) shows that SEM image of nickel ferrite at 600°C sintering temperature. It is clearly observed from the image they are agglomerated, highly branched and porous in nature. The average grain size was calculated by using line intercept formula and it is found to be 0.21μm.

AC Conductivity

Using the values of equivalent parallel capacitance (Cp), dissipation factor (D), phase angle (δ) and parallel equivalent resistance (Rp) that are recorded by the LCR meter at selected frequency range (*f*), the ac conductivity (σ_{ac}), dielectric constant (ε′) and dielectric loss (tan δ) parameters have been calculated [15].

The resistance ρ_{ac} of the samples was found by using the equation.

$$\rho_{ac} = \frac{R_P \ x \ A}{t} \qquad (1)$$

Where R_p, the resistance of the sample is given by,

$$R_p = Z\sqrt{(1+\tan\phi)^2} \qquad (2)$$

The a.c conductivity is frequency and temperature dependent entity. The electrical conduction is a thermally activated process and follows the Arrhenious law

$\sigma_{ac} = \sigma_0 e^{-Ea/KT}$ where σ_{ac} conductivity, σ_0 is pre exponential factor, E_a is the activation energy and K is Boltzmann constant.

The ac conductivity σ_{ac} was determined using the formula

$$\sigma_{ac} = \frac{1}{\rho_{ac}} \qquad (3)$$

When field is applied to a dielectric, the polarization of the dielectric takes place. The dielectric displacement found in a dielectric material when subjected to an alternating field (E) is not in phase. Hence the dielectric constant is a complex quantity and is expressed as

$$\varepsilon^* = \varepsilon' + i\varepsilon'' \qquad (4)$$

where ε′ is the real part (denoted as ε_r for our discussions) and ε″ is the imaginary part,

In the rectangular coordinate system, the real and imaginary part of the impedance was calculated by formulae

$$Z' = |Z| \cos\phi \qquad (5)$$

When the complex impedance plane plots were obtained, where a semicircle, is obtained the relaxation time was calculated using the relation ωτ=1.

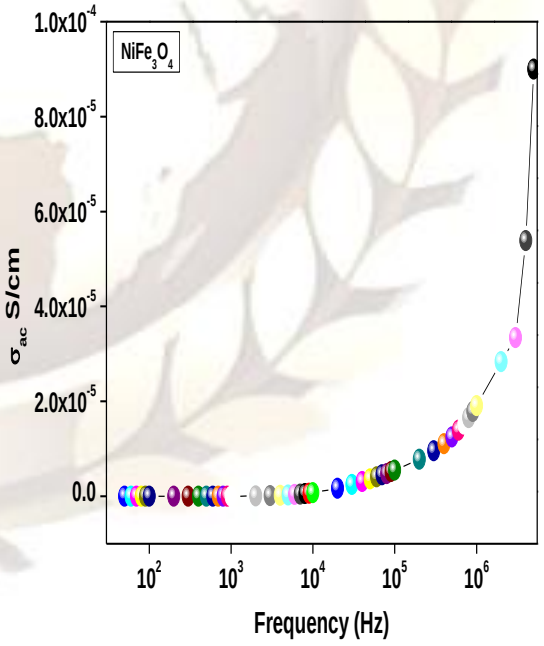

Figure 3. Shows the variation of σ_{ac} of $NiFe_3O_4$ as a function of frequency.

Figure 3 shows the variation of σ_{ac} of $NiFe_3O_4$, as a function of frequency. The conductivity of nickel ferrites is increases with increase in frequency. The nickel ferrite ($NiFe_3O_4$) shows σ_{ac} conductivity of 1.0 x 10^{-4} S/cm. This is may be attributed to the dipole polarization i.e., the rotation of dipoles between two equivalent equilibrium positions is involved. It is the spontaneous alignment of dipoles in one of the equilibrium positions that give rise to the nonlinear polarization behavior of this composition.

This behavior of $NiFe_3O_4$ obeys the universal power law, $\sigma(\omega)=\sigma_0 + A(\omega)^n$ (the solid line is the fit to the expression), where r0 is the dc conductivity (frequency independent plateau in the low frequency region), A is the pre-exponential factor, and n is the fractional exponent between 0 and 1 [16]. On crystallization, the conductivity spectrum remains similar as that of the nickel ferrite except dispersion in the low frequency region, where the deviation from σ_{dc} (plateau region) is more prominent. The deviation from σ_{dc} (plateau region) value in the conductivity spectrum (in the low frequency region) is due to the electrode polarization effect. The values of σ, A, and n were obtained by fitting the $\sigma(\omega)$ to $\sigma(\omega)=\sigma_0 + A(\omega)^n$. The overall behavior of σ_{ac} follows the universal dynamic response, which has widely been observed in disordered materials like ionically conducting glasses and also doped crystalline solids, and is generally believed to be reflected in the mechanism of charge transport behavior of charge carriers.

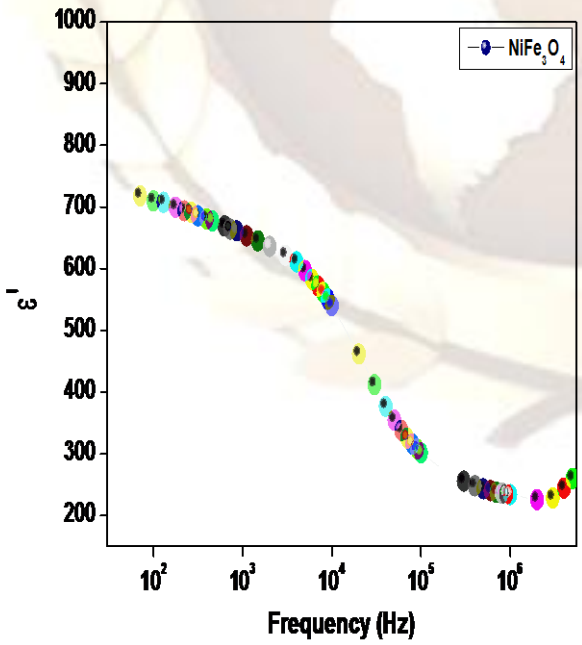

Figure 4. Shows the variation real permittivity (ε') of nickel ferrite as a function of frequency.

Figure 4 shows the variation real permittivity (ε') of nickel ferrite of various composition as a function of logarithmic frequency. It is found that in all these nickel ferrite compositions, as frequency increases, dielectric constant decreases up to the frequency range of 10^4 Hz and after that it remains constant for further increasing in frequency. The strong frequency dispersion of permittivity is observed in the low frequency region followed by a nearly frequency independent behavior above 10 kHz. It is observed that Debye type relaxation mechanism is responsible for higher value of $NiFe_3O_4$.

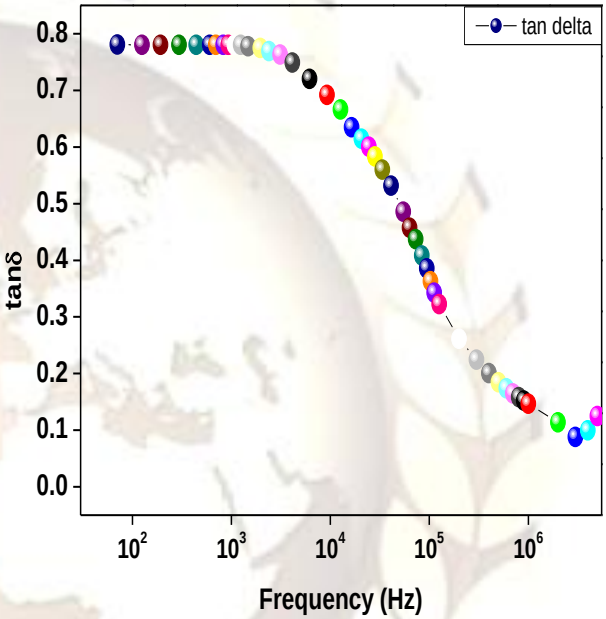

Figure 5. Shows the variation of dielectric constant as a function of frequency of $NiFe_3O_4$

Figure 5 shows the variation of dielectric constant as a function of frequency for $NiFe_3O_4$. The high value of dielectric constant of the sample $NiFe_3O_4$ may be explained on the basis of the structural changes associated with the nickel ferrite when the grain size is reduced to nanometer order. Nickel ferrite crystallizes into a cubic close-packed arrangement of oxygen ions. It belongs to the class of ferrites with an inverse spinel structure having structural formula, $Fe^{3+}[Ni^{2+}Fe^{3+}]O_4$. The metal ions given in the square bracket are called octahedral (B site) ions and that outside the square bracket are called tetrahedral (A site) ions. The nickel ions (Ni^{2+}) together with half of the iron ions (Fe^{3+}) occupy the B site and the remaining half of the iron ions reside in A site. The presence of Ni^{2+} and Ni^{3+} ions gives rise to p-type carriers (holes) whereas Fe^{2+} and Fe^{3+} ions produce n-type carriers (electrons). Therefore, both electrons and holes that are present in the B sites are due to the presence of Ni and Fe ions.

Since only iron ions are present in A sites, electrons are the carriers in A sites. The distance between the ions in A sites (0·357 nm) is larger than the distance between the ions in B site (0·292 nm). Also, the degree of covalency for the A site ions is higher than that of the B site ions. All the above factors result in a high activation energy for the A sites compared to the B sites. Hence, in ordinary nickel ferrite with an inverse spinel structure the electron movement in B sites dominates compared to that in A sites.

Conclusion

Nickel ferrite ($NiFe_3O_4$) is prepared by employing sol gel technique. XRD studies revels that the percentage of iron ions in B site increases with the reduction in grain size. This shifting of ions causes changes in XRD pattern also. As the percentage of iron ions in B site increases, the intensity of the (222) peak compared to that of the (220) peak increases. From the SEM image, it is observed that the granular size increases with increase in percentage of Ni and sintering temperature. The nickel ferrite shows high σ_{ac} conductivity of 1.3×10^{-4} S/cm due to attribution of the dipole polarization. The high value of dielectric constant of the sample $Ni_XFe_{X-1}O_4$ is because of structural changes associated with the nickel ferrite when the grain size is reduced to nanometer order.

Reference

[1] D. Vladikova, H. Yonchev, L. Ilkov, S. Karbanov, J. Magn. Magn. Mater. 78 (1989) 420
[2] A.M. El-Sayed, Materials Chemistry and Physics 82 (2003) 583–587
[3] J . S . Baijal, deepika kothari and sumitra phanjoubam, Proceedings of ICF-5 (1989) pp. 371.
[4] J . Smit, "Magnetic Properties of Materials" (Mc Grow-hill Book Company, New York, 1971).
[5] K. J . Standley, "Oxide Magnetic Materials" (Oxford UK Clarendon, 1972).
[6] M. I . Rosales, E. Amano, M. P . Cuatle and R. Valenzuela, Mater. Sci. Engng. B49 (1997) 221.
[7] K. C. Patil, S . Sunder manoharan and D. Gajpathy, Marcel Deekar 1 (1990) 473.
[8] A. Verma, T. C. Goel, R. G. Mendiratta and R. G. Gupta, Journal of Magnetism and Magnetic Materials 192(1999) 271.
[9] A. Verma, T. C. Goel, R. G. Mendiratta and P . Kishan, ibid. 208 (2000) 13.
[10] C. N. R. Rao and J . Gopalkrishnan, "New Directions in Solid State Chemistry" (Cambridge Univ. Press, (1989).
[11] Giannakopoulou T, Kompotiatis L, Kontogeorgakos A and Kordas G 2002 J. Magn. Magn. Mater. 246 360
[12] Goldman A 1990 Modern ferrite technology (New York: Van Nostrand Reinhold) p. 71
[13] Gopal Reddy C V, Manorama S V and Rao V J 1999 Sensors and Actuators B55 90
[14] Gotic M, Czako-Nagy I, Popovic S and Music S 1998 Philos. Mag. 78 193
[15] Green J J, Waugh J S and Healy B J 1964 J. Appl. Phys. 35 1006
[16] Han K C, Choi H D, Moon T J and Kim W S 1995 J. Mater. Sci. 30 3567